A Letters Journal Exploring the Frontiers of Physics

October 2009

EPL, **88** (2009) 11001
doi: 10.1209/0295-5075/88/11001

www.epljournal.org

NLO-QCD corrections to Wγj production

F. Campanario[1,2], C. Englert[1(a)], M. Spannowsky[1] and D. Zeppenfeld[1]

[1] *Institute for Theoretical Physics, University of Karlsruhe, KIT - 76128 Karlsruhe, Germany, EU*
[2] *Departament de Física Teòrica and IFIC, Universitat de València - CSIC - E-46100 Burjassot, València, Spain, EU*

received 19 August 2009; accepted in final form 23 September 2009
published online 23 October 2009

PACS 12.38.Bx – Perturbative calculations
PACS 13.85.-t – Hadron-induced high- and super-high-energy interactions (energy > 10 GeV)
PACS 14.70.Bh – Photons

Abstract – We calculate the $W^{\pm}\gamma j + X$ production cross-sections at next-to-leading-order QCD for Tevatron and LHC collisions. We include leptonic decays of the W to light leptons, with all off-shell effects taken into account. The corrections are sizable and have significant impact on the differential distributions.

Introduction. – At hadron colliders such as the CERN Large Hadron Collider (LHC) and the Fermilab Tevatron, electroweak boson production in association with jets represents important signal processes as well as backgrounds to future searches beyond the Standard Model (BSM). One example is the measurement of anomalous triboson couplings, arising from BSM physics, which can be obscured by higher-order QCD effects. For these searches, significance-improving strategies include jet vetos, which amount to subtraction of a leading-order cross-section [1], and are plagued at present with typical QCD scale uncertainties. Improved QCD precision of production cross-sections is therefore essential and has been agreed on as a common goal of precision phenomenology in the so-called "Les Houches wish-list" [2]. Considerable progress in completing this task has been accomplished, cf. [3–7]. Concerning electroweak boson production in association with a jet, the QCD corrections to W^+W^- + jet have been recently provided in [5].

In this letter we examine $W^{\pm}\gamma$ + jet production at next-to-leading-order (NLO) QCD, including leptonic decays of the $W^{\pm}$. We devote special care to the development of a fully flexible, numerically stable parton level Monte Carlo implementation, based on the Vbfnlo framework [8]. Although full leptonic decays of the massive $W^{\pm}$ are included, we will refer to the processes as $W^{\pm}\gamma j$ production in the following.

Elements of the calculation and checks. – The leading-order contribution, at $\mathcal{O}(\alpha^3\alpha_s)$, to the process $pp \to \ell^-\bar{\nu}_\ell\gamma j + X$ includes subprocesses of the type

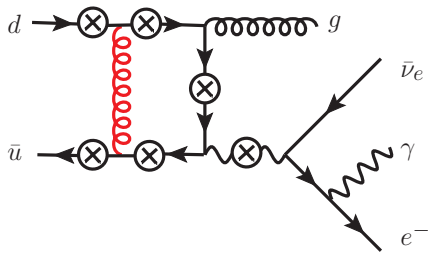

Fig. 1: (Colour on-line) Representative Feynman graph contributing to the virtual corrections to the partonic subprocess $\bar{u}d \to e^-\bar{\nu}_e\gamma g$ at $\mathcal{O}(\alpha^3\alpha_s^2)$. The crosses mark other points where the photon is attached to the quark line and the W boson.

$q\bar{Q} \to \ell^-\bar{\nu}_\ell\gamma g$, and qg and $\bar{Q}g$ initiated subprocesses which are related by crossing.

The 10 Feynman graphs of each subprocess can be classified into two categories: First, configurations where the photon is emitted from the W or the W's decay lepton, and, second, graphs where the photon is emitted from the quark line. Performing the virtual correction at $\mathcal{O}(\alpha^3\alpha_s^2)$, these topologies give rise to self-energy, triangle, box, and pentagon (sub-)diagrams, fig. 1. The loop corrections are treated using standard methods: self-energy, triangle, box and pentagon integrals are evaluated in terms of tensor coefficients [9,10] in dimensional reduction, after having applied $\overline{\text{MS}}$ renormalization. We combine the virtual corrections to groups that include all loop diagrams derived from a Born level configuration, *i.e.* all self-energy, triangle, box and pentagon corrections to a quark line with three attached gauge bosons are combined to a single routine. This method leaves us with a universal set of

(a) E-mail: englert@particle.uni-karlsruhe.de

virtual building blocks, which are then assembled for the specific process under consideration. This strategy has already been applied to various phenomenological studies at NLO-QCD precision, *e.g.* [6,11].

The reduction of the loop diagrams has been calculated in two independent ways for verification reasons. The first approach uses in-house routines within in the framework of FeynCalc [12] and FeynArts, while the second one relies on FeynArts, FormCalc, and LoopTools [13,14], with modifications, in particular to the treatment of divergencies, as described in [15]. We find that both calculations numerically agree within Fortran precision for different phase space points. Performing the NLO computation in the chiral limit, the arising infrared (IR) singularities have been determined separately in independent approaches, and checked against existing results in the literature [16,17].

The IR singularities encountered in the real emission contributions are regularized using the Catani-Seymour dipole formalism [18]. The numerical implementation of the dipoles has been numerically checked against MadDipoles [19]. The code is optimized such that intermediate dipole results are stored and reused in order to avoid redundant calculations. Remaining finite collinear terms, after renormalizing the parton distribution functions according to [18], were analytically calculated in two independent ways. We integrate the finite collinear terms over the real emission phase space by appropriately mapping the LO phase space, as done in [20]. The cancellation of virtual IR singularities against the one-parton phase-space–integrated dipoles has been checked analytically.

We evaluate the leading-order matrix element, as well as the subtraction terms using partly modified Helas routines [21] generated with MadGraph [22]. Due to the increase of subprocesses when going to the evaluation of the IR-subtracted real emission matrix element, optimization is imperative in order not to jeopardize CPU time. Here, the matrix element is calculated using the spinor helicity formalism of [23], and intermediate numerical results, common to all subprocesses, are stored and reused, thus speeding up the numerical code. The real emission matrix elements, cf. fig. 2 for sample graphs of the partonic subprocess $\bar{u}d \to e^- \bar{\nu}_e \gamma gg$, have been checked numerically against code generated by MadGraph for every subprocess. Integrated results were checked against Sherpa [24]. Table 1 representatively gives the result of our comparison of integrated cross-sections with MadEvent v4.2.21 and Sherpa v.1.1.3 for the leading-order and the real emission dijet contribution, *i.e.* the process $pp \to e^- \bar{\nu}_e \gamma jj + X$ at $\mathcal{O}(\alpha^3 \alpha_s^2)$, for cuts specified below.

Concerning the Monte Carlo implementation of the virtual corrections, we have implemented the loop contributions using our VBFNLO routines, that involve the Passarino-Veltman reduction scheme [9] up to boxes, the Denner-Dittmaier reduction scheme [10] for pentagons,

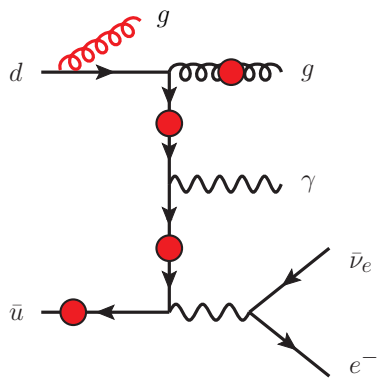

Fig. 2: (Colour on-line) Sample Feynman graph contributing to the partonic real emission subprocess $\bar{u}d \to e^- \bar{\nu}_e \gamma gg$ at $\mathcal{O}(\alpha^3 \alpha_s^2)$. The gluon is attached to the quark and gluon lines at positions marked by the circles. Feynman graph topologies, where the photon is radiated off at different positions analogous to fig. 1, are not shown.

Table 1: Comparison of integrated $W^-\gamma j$ and $W^-\gamma jj$ tree level cross-sections at the LHC. The cross-sections were calculated with our modified version of VBFNLO, MadEvent v4.4.21, and Sherpa v.1.1.3. The QCD-IR-safe photon isolation is replaced by a conventional separation $R_{j\gamma} \geqslant 1$ for all jets. We also require $R_{\ell\gamma} \geqslant 0.4$ and $R_{jj} \geqslant 0.7$. All other parameters and cuts are chosen as described in the text.

	$W^-\gamma j$ [fb]	$W^-\gamma jj$ [fb]
mod. VBFNLO	268.38 ± 0.12	124.74 ± 0.10
Sherpa	268.14 ± 0.37	124.35 ± 0.59
MadEvent	268.24 ± 0.69	123.80 ± 0.40

and the spinor helicity formalism of [23]. Throughout, the numerical integration is performed using a modified version of Vegas [25], which is part of the VBFNLO package, with different channels for the two- and three-body decay of the W boson. Finite width effects of the W boson are taken into account using a modified version of the complex mass scheme of [26]: the weak mixing angle is taken to be real, while using a Breit-Wigner propagator for the W boson. This scheme corresponds to the implementation in MadGraph.

For a more detailed discussion of the calculation and its numerical implementation, we refer the reader to a separate paper [27].

Numerical results. – We use CTEQ6M parton distributions [28] with $\alpha_s(m_Z) = 0.118$ at NLO, and the CTEQ6L1 set at LO. We choose $m_Z = 91.188\,\text{GeV}$, $m_W = 80.419\,\text{GeV}$ and $G_F = 1.16639 \times 10^{-5}\,\text{GeV}^{-2}$ as electroweak input parameters and derive the electromagnetic coupling α and the weak mixing angle $\sin\theta_w$ via Standard Model-tree level relations. The center-of-mass energy is fixed to 14 TeV for LHC and 1.96 TeV for Tevatron collisions, respectively. We only consider $W^\pm$ decays to one family of light leptons, *e.g.* $W^- \to e^- \nu_e$, and treat these leptons as massless. The

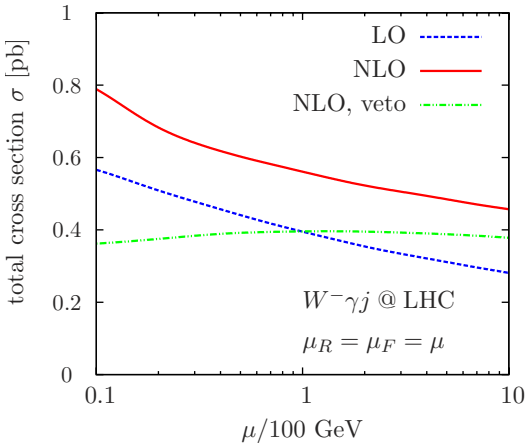

Fig. 3: (Colour on-line) Comparison of the scale dependence of the total cross-section of $pp \to e^- \bar{\nu}_e \gamma j + X$ at LO (dashed line), NLO-QCD (solid line), and NLO-QCD with the second jet vetoed (dot-dashed line) for the cuts chosen as described in the text at the LHC.

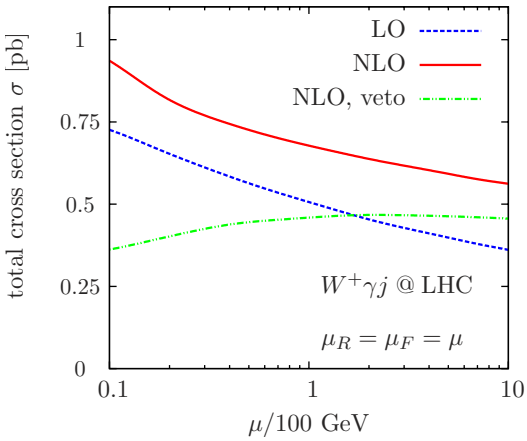

Fig. 4: (Colour on-line) Comparison of the scale dependence of the total cross-section of $pp \to e^- \bar{\nu}_e \gamma j + X$ at LO (dashed line), NLO-QCD (solid line), and NLO-QCD with the second jet vetoed (dot-dashed line) for the cuts chosen as described in the text at the LHC.

CKM-matrix is taken to be diagonal, and we neglect bottom contributions throughout. A non-diagonal CKM-matrix decreases our leading-order LHC result at the per mill level as gluon-induced processes dominate the cross-section. The correction for the Tevatron results, which are mostly quark induced, is about 3%. These corrections are well below the residual scale dependence at NLO-QCD. The bottom contributions are negligible and can be further suppressed by b-tagging. Jets are recombined via the k_T algorithm [29] from massless partons of pseudorapidities $|\eta| \leqslant 5$ with resolution parameter $D = 0.7$. The jets are required to lie in the rapidity range $|y_j| \leqslant 4.5$ with $p_T^{\text{jet}} \geqslant 50\,\text{GeV}$. The photon and the charged lepton are chosen to be rather hard and central, $p_T^\ell \geqslant 20\,\text{GeV}$, $p_T^\gamma \geqslant 50\,\text{GeV}$, $|\eta_\ell|, |\eta_\gamma| \leqslant 2.5$, while being separated in the azimuthal angle-pseudorapidity plane by $R_{\ell\gamma} = (\Delta\phi_{\ell\gamma}^2 + \Delta\eta_{\ell\gamma}^2)^{1/2} \geqslant 0.2$. For the separation of the charged lepton from observable jets, we choose $R_{\ell j} \geqslant 0.2$. A naive isolation criterion for the partons and the photon spoils IR safety, yet isolation is necessary to avoid fragmentation contributions. We apply the method suggested in [30], demanding

$$\sum_{i, R_{i\gamma} < R} p_T^{\text{parton},i} \leqslant \frac{1 - \cos R}{1 - \cos \delta_0}\, p_T^\gamma, \qquad \forall R \leqslant \delta_0, \qquad (1)$$

where the index i runs over all partons, found in a cone around the photon of size R. For the cut-off parameter, that determines the QCD-IR-safe cone size around the photon, we choose $\delta_0 = 1$.

At leading order, we find a QCD scale dependence of approximately 11% for $W^\pm\gamma j$ production at the LHC, when varying $\mu_R = \mu_F$ by a factor two around 100 GeV, cf. figs. 3 and 4 for identified renormalization and factorization scales. This scale dependence is only reduced to about 7% when including NLO-QCD precision for $W^\pm\gamma j$. This is due to the renormalization scale dependence of the dijet contribution at NLO. Vetoing additional jets results in a stabilization of the cross-section, as the veto projects on true $W^\pm\gamma j$ events. This agrees with the results on $W^+W^- j$ production [5] and $W^\pm\gamma$ production [1,31].

Table 2: Next-to-leading-order cross-sections and K-factors for the processes $pp \to W^\pm\gamma j + X$ at the LHC for identified renormalization and factorization scales, $\mu_R = \mu_F = 100\,\text{GeV}$. The cuts are chosen as described in the text.

	σ^{NLO} [fb]	$\sigma^{\text{NLO}}/\sigma^{\text{LO}}$
$W^-\gamma j$	558.7 ± 2.4	1.413
$W^+\gamma j$	676.9 ± 3.2	1.339

The difference of $W^+\gamma j$ compared to $W^-\gamma j$ is predominantly due to the different parton distribution functions of the dominant subprocesses. Qualitatively, the findings of the $W^-\gamma j$ channel generalize to $W^+\gamma j$, accompanied by an overall increase of the cross-section of about 54% (see also table 2).

At the Tevatron, fig. 5, we find a LO scale dependence of 23%, which is reduced to about 8% at NLO-QCD. A jet veto is not necessary to stabilize the perturbative corrections as additional jet radiation is sufficiently suppressed by the hard cut on the jet transverse momentum, $p_T^{\text{jet}} \geqslant 50\,\text{GeV}$.

For the scale choice $\mu = 100\,\text{GeV}$ the total NLO result differs by about 41% for $W^-\gamma j$ from the total LO cross-section. As usual, however, the total K-factor, defined to be $K = \sigma^{\text{NLO}}/\sigma^{\text{LO}}$, reflects only partly the impact of the QCD quantum corrections on the entire processes' characteristics. Quantitative understanding thereof can be gained from differential K-factors of (IR-safe) observables $\mathcal{O}$,

$$K(\mathcal{O}) = \frac{\mathrm{d}\sigma^{\text{NLO}}}{\mathrm{d}\mathcal{O}} \Big/ \frac{\mathrm{d}\sigma^{\text{LO}}}{\mathrm{d}\mathcal{O}}.$$

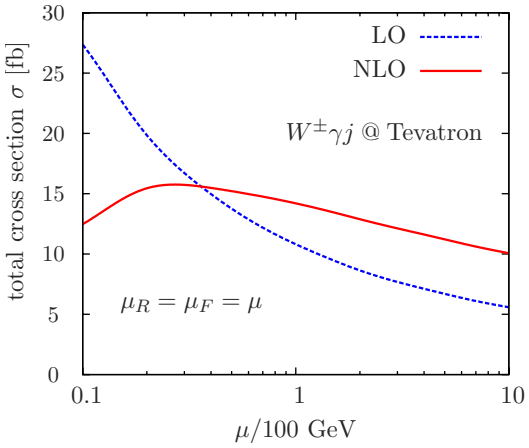

Fig. 5: (Colour on-line) Tevatron comparison of the scale dependence of the total cross-section of $p\bar{p} \to e^- \bar{\nu}_e \gamma j + X$ or $p\bar{p} \to e^+ \nu_e \gamma j + X$ at LO (dashed line) and NLO-QCD (solid line) for the cuts chosen as described in the text.

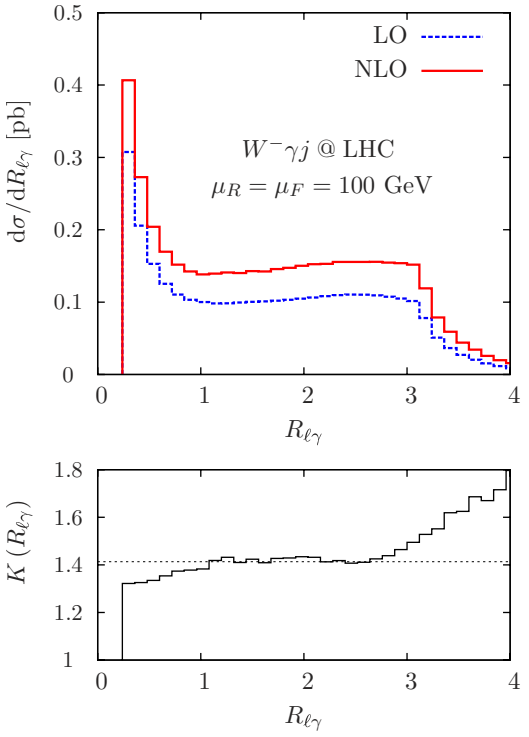

Fig. 6: (Colour on-line) Differential distribution of the photon-lepton separation $R_{\ell\gamma}$ at LO (dashed line) and at NLO (solid line). The lower panel shows the differential K-factor. The dotted line denotes the total K-factor of table 2.

In figs. 6 and 7, we representatively show the lepton-photon separation and the p_T-spectrum of the hardest jet at LO and NLO, accompanied by the respective differential K-factors. The distributions develop significant changes when including NLO-QCD precision, yielding large relative modifications around the total K-factor.

Summary and Outlook. – We have presented first results on the NLO-QCD corrections to $pp \to W^{\pm}\gamma j + X$ and $p\bar{p} \to W^{\pm}\gamma j + X$, including leptonic decays and full off-shell effects for the W boson. The calculation has been implemented in a parton level Monte Carlo program based on the VBFNLO framework which, thus, is fully flexible except for the limitation that the Frixione definition of photon isolation as given in eq. (1) must be used. Using this program, we give sample results for total next-to-leading-order cross-sections, as well as differential distributions and differential K-factors.

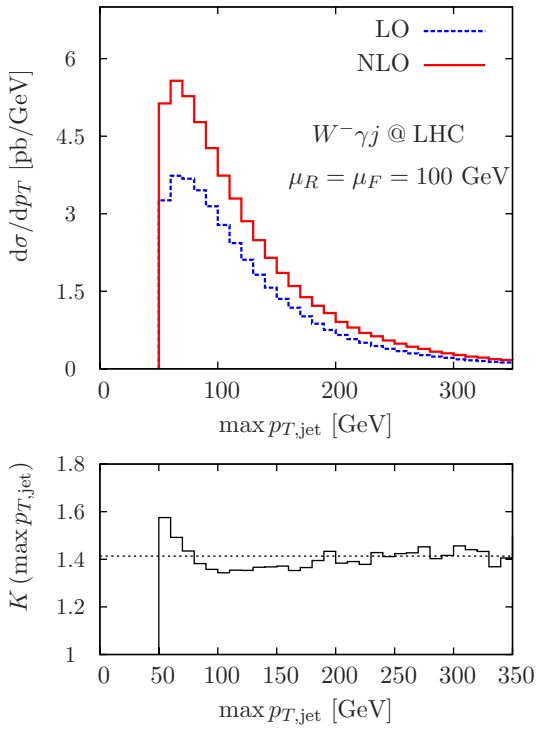

Fig. 7: (Colour on-line) Maximum jet-p_T distribution at leading order (dashed line) and next-to-leading-order QCD (solid line). The dotted line denotes the total K-factor of table 2.

We find a fairly reduced scale dependence of the total cross-sections, cf. figs. 3–5, for a fixed scale choice $\mu_F = \mu_R = \mu$ and our cuts. The corrections turn out to be sizable, around 41% for $W^-\gamma j$ production and 34% for $W^+\gamma j$ production at the LHC. The total correction at the Tevatron is about 30%.

These total corrections are accompanied by significant modifications of up to 60% for differential distributions when going from LO to NLO, figs. 6 and 7.

A more detailed investigation, including analysis of the impact of anomalous couplings and the calculation of NLO-QCD jet veto efficiencies for searches suggested in [1], is underway. Eventually, this process will be made publicly available as part of the VBFNLO package.

* * *

We would like to thank S. DITTMAIER, S. KALLWEIT and G. BOZZI for helpful discussions, and S. SCHUMANN for SHERPA support. FC acknowledges a postdoctoral

fellowship of the Generalitat Valenciana "Beca Postdoctoral d'Excel.lència" and CE is supported by "KCETA Strukturiertes Promotionskolleg". This research is partly funded by the Deutsche Forschungsgemeinschaft under SFB TR-9 "Computergestützte Theoretische Teilchenphysik", European FEDER and Spanish MICINN under grant FPA2008-02878, and the Helmholtz alliance "Physics at the Terascale".

REFERENCES

[1] Baur U., Han T. and Ohnemus J., *Phys. Rev. D*, **48** (1993) 5140 (arXiv:hep-ph/9305314).
[2] Buttar C. *et al.*, arXiv:hep-ph/0604120.
[3] Binoth T., Ossola G., Papadopoulos C. G. and Pittau R., *JHEP*, **0806** (2008) 082 (arXiv:0804.0350).
[4] Bredenstein A., Denner A., Dittmaier S. and Pozzorini S., *Phys. Rev. Lett.*, **103** (2009) 012002 (arXiv:0905.0110).
[5] Dittmaier S., Kallweit S. and Uwer P., *Phys. Rev. Lett.*, **100** (2008) 062003 (arXiv:0710.1577); Campbell J. M., Keith Ellis R. and Zanderighi G., *JHEP*, **0712** (2007) 056 (arXiv:0710.1832).
[6] Campanario F., Hankele V., Oleari C., Prestel S. and Zeppenfeld D., *Phys. Rev. D*, **78** (2008) 094012 (arXiv:0809.0790).
[7] Bevilacqua G., Czakon M., Papadopoulos C. G., Pittau R. and Worek M., arXiv:0907.4723 [hep-ph].
[8] Arnold K. *et al.*, *Comput. Phys. Commun.*, **180** (2009) 1661 (arXiv:0811.4559).
[9] Passarino G. and Veltman M. J. G., *Nucl. Phys. B*, **160** (1979) 151.
[10] Denner A. and Dittmaier S., *Nucl. Phys. B*, **658** (2003) 175 (arXiv:hep-ph/0212259); **734** (2006) 62 (arXiv:hep-ph/0509141).
[11] Bozzi G., Jager B., Oleari C. and Zeppenfeld D., *Phys. Rev. D*, **75** (2007) 073004 (arXiv:hep-ph/0701105); Hankele V. and Zeppenfeld D., *Phys. Lett. B*, **661** (2008) 103 (arXiv:0712.3544); Englert C., Jager B. and Zeppenfeld D., *JHEP*, **0903** (2009) 060 (arXiv:0812.2564).
[12] Mertig R., Bohm M. and Denner A., *Comput. Phys. Commun.*, **64** (1991) 345.
[13] Hahn T. and Perez-Victoria M., *Comput. Phys. Commun.*, **118** (1999) 153 (arXiv:hep-ph/9807565).
[14] Hahn T., *Comput. Phys. Commun.*, **140** (2001) 418 (arXiv:hep-ph/0012260).
[15] Bredenstein A., Denner A., Dittmaier S. and Pozzorini S., *JHEP*, **0808** (2008) 108 (arXiv:0807.1248).
[16] Dittmaier S., *Nucl. Phys. B*, **675** (2003) 447 (arXiv:hep-ph/0308246).
[17] Figy T., Hankele V. and Zeppenfeld D., *JHEP*, **0802** (2008) 076 (arXiv:0710.5621).
[18] Catani S. and Seymour M. H., *Nucl. Phys. B*, **485** (1997) 291; **510** (1998) 503(E) (arXiv:hep-ph/9605323).
[19] Frederix R., Gehrmann T. and Greiner N., *JHEP*, **0809** (2008) 122 (arXiv:0808.2128).
[20] Figy T., Oleari C. and Zeppenfeld D., *Phys. Rev. D*, **68** (2003) 073005 (arXiv:hep-ph/0306109).
[21] Murayama H., Watanabe I. and Hagiwara K., KEK-Report 91-11, 1992.
[22] Alwall J. *et al.*, *JHEP*, **0709** (2007) 028 (arXiv:0706.2334).
[23] Hagiwara K. and Zeppenfeld D., *Nucl. Phys. B*, **313** (1989) 560.
[24] Gleisberg T., Hoche S., Krauss F., Schonherr M., Schumann S., Siegert F. and Winter J., *JHEP*, **0902** (2009) 007 (arXiv:0811.4622).
[25] Lepage G. P., *J. Comput. Phys.*, **27** (1978) 192.
[26] Denner A., Dittmaier S., Roth M. and Wackeroth D., *Nucl. Phys. B*, **560** (1999) 33 (arXiv:hep-ph/9904472); Oleari C. and Zeppenfeld D., *Phys. Rev. D*, (69) 2004093004 (arXiv:hep-ph/0310156).
[27] Campanario F., Englert C., Spannowsky M. and Zeppenfeld D., in preparation.
[28] Pumplin J., Stump D. R., Huston J., Lai H. L., Nadolsky P. and Tung W. K., *JHEP*, **0207** (2002) 012 (arXiv:hep-ph/0201195).
[29] Catani S., Dokshitzer Y. L., Seymour M. H. and Webber B. R., *Nucl. Phys. B*, **406** (1993) 187.
[30] Frixione S., *Phys. Lett. B*, **429** (1998) 369 (arXiv:hep-ph/9801442).
[31] Dixon L. J., Kunszt Z. and Signer A., *Phys. Rev. D*, **60** (1999) 114037 (arXiv:hep-ph/9907305).